Spectrum and dynamic-response function of transmitted light in the absorptive optical bistability

Peter Hänggi, Adi R. Bulsara, Ralph Janda

Angaben zur Veröffentlichung / Publication details:

Hänggi, Peter, Adi R. Bulsara, and Ralph Janda. 1980. "Spectrum and dynamic-response function of transmitted light in the absorptive optical bistability." *Physical Review A* 22 (2): 671–83. https://doi.org/10.1103/physreva.22.671.

PHYSICAL REVIEW A VOLUME 22, NUMBER 2 AUGUST 1980

Spectrum and dynamic-response function of transmitted light in the absorptive optical bistability

Peter Hanggi and Adi R. Bulsara
Department of Chemistry, University of California, San Diego, La Jolla, California 92093

Ralph Janda
Physical Dynamics, Inc., P. O. Box 1883, La Jolla, California 92038

(Received 5 November 1979)

We consider the dynamical behavior of the (nonlinear) amplitude fluctuations in the transmitted radiation of the optical bistability in the transition region. A Fokker-Planck model with nonlinear diffusion coefficient (multiplicative Gaussian white noise) is used to describe the system in the "good-quality" cavity limit. Choosing a parameter set corresponding to a numerically small but tractable tunneling rate between the stable and metastable states we study, as functions of the external coherent field and system size, the spectrum and the response to a small additional injected coherent signal. The numerical calculations are facilitated by the construction of complex-valued continued-fraction representations for the spectrum of amplitude fluctuations and for the response function. This representation allows us to discuss the memory effects caused by deviations from a simple Gaussian-Markov behavior around the transition region. In addition, such a representation enables the construction of *"a posteriori"* error bounds on the power spectrum.

I. INTRODUCTION

The phenomenon of the absorptive optical bistability (OB) has recently attracted a great deal of interest as a clear example of spontaneous ordering in a stationary system far from thermal equilibrium. The OB was first predicted by Szoke *et al.*[1] and subsequently studied theoretically by a number of authors,[2] both from a semiclassical as well as from a fully quantum-statistical point of view. The fundamental feature described by them is that the transmitted light from a system of two-level atoms in a cavity driven by a coherent, quasiresonant external field varies discontinuously, exhibiting the characteristics of a first-order transition, a hysterisis cycle, that was first observed experimentally by Gibbs *et al.*[3] These experiments revealed a wide range of possible applications of the OB as an optical transistor, optical memory element, pulse shaper, etc., and stimulated a very active, still increasing interest in the phenomenon.[4]

It is customary (and convenient) to treat the OB in a mean-field[2(b),2(c),2(e)] approximation which amounts to requiring that the field be sufficiently uniform over the length of the active volume. The limits of validity of this type of approach have been examined in Ref. 5. Most of the present research is limited to the statistical mechanics of the static behavior of the instability. One of the challenges addressed by this paper is a study of the dynamics of the OB such as the calculation of the spectrum of the transmitted light and the response function in the regime of a multiplicity of possible stationary states. For the spectrum of the transmitted light, this problem has been considered in the recent work of Lugiato[6] and Agarwal *et al.*[7] using either an approach via the Fokker-Planck equation linearized about a steady state or an equivalent approach based on a system-size expansion as developed for classical stochastic systems.[8] These methods amount to treating the stable and metastable states on the same footing, thereby assuming a very large (thus physically irrelevant) transition time.

However, both these approaches work well only in a regime of parameter values for which the fluctuations obey Gaussian-Markov statistics. Further, in order to calculate the *true* spectrum of the stationary fluctuations, the relative weights of the different locally stable states as well as the time scale of the tunneling between different locally stable semiclassical stationary states becomes important. If the time scale of the tunneling from one semiclassical stationary state to the other is not extremely large (corresponding to a small system size), the approaches mentioned above cannot be used.[9] (In this case it is necessary to use an asymptotic expansion for the process which incorporates the characteristics of the stable as well as of the metastable state.)

The purpose of this paper is to investigate the dynamics of the OB in the case of a "good-quality" cavity in which the empty cavity width is much smaller than the atomic linewidth. We study the statistical properties of the amplitude fluctuations for parameter values for which a non-Gaussian statistical behavior as well as a numerically small

but tractable tunneling rate play important roles. In doing so, we shall use a continued fraction representation for the various dyanmic correlation functions. This continued fraction representation allows further a construction scheme of *"a posteriori"* error bounds[10] for the frequency-dependent transport properties which are not known exactly.

The outline of the paper is the following. In Sec. II, we present a simplified Fokker-Planck model of a mean-field description for the amplitude fluctuations in the OB for the case of a good-quality cavity, this model having been originated in the work of Refs. 2(e) and 11. We present the stationary dynamics of our chosen set of parameters and discuss some asymptotic properties of the stationary probability as a function of the system size (number of atoms). In principle, the correct dynamic statistics of the amplitude fluctuations $\delta x(t)$ may be obtained by performing an exact coarse-graining over the phase fluctuations ($\delta\phi$) in a Markovian master equation for the joint process $z(t)=[x(t),\phi(t)]$. This would lead to a non-Markovian dynamics.[12] In Sec. II, we give a discussion of the physical time scales with the conclusion that, for our chosen set of parameters, the difference in the time scales for the amplitude and phase fluctuations is sufficiently large so that the Fokker-Planck model of the amplitude fluctuations is a good approximation. The response of the system to a small additional time-dependent modulated quasiresonant coherent signal is investigated in Sec. III. In Sec. IV we elaborate on the calculation of dynamical correlations in terms of continued fractions (the first six continued-fraction coefficients are given in the Appendix, these being expressed solely in terms of static quantities). As a result of the deviation from a simple Lorentzian behavior, the continued fraction coefficients c_n for $n>2$ describe memory effects,[13] these being most pronounced in the regime of a multiplicity of stationary states. The results of the numerical calculations for the spectrum of the transmitted light and for the complex susceptibility are given in Sec. V.

II. FOKKER-PLANCK MODEL FOR AMPLITUDE FLUCTUATIONS IN THE OPTICAL BISTABILITY

We consider a homogeneously broadened active medium of length L and volume V composed of $N \gg 1$ two-level atoms of transition frequency ω_0, enclosed in a resonant ring cavity with transmission coefficient T. This cavity is then placed in a ring laser cavity. A classical real, positive, and coherent resonant signal of amplitude $E_I=\alpha\sqrt{T}$ is injected into the cavity in the longitudinal direction, thereby inducing a macroscopic atomic polarization S. The system may then be described in a semiclassical mean-field approximation in terms of the (resonant) single-mode Bloch-Maxwell equations[2(b)]

$$\dot{S}=2gb\sigma-\gamma_\perp S, \tag{2.1a}$$

$$\dot{\sigma}=-2gbS-\gamma_\parallel(\sigma-N/2), \tag{2.1b}$$

$$\dot{b}=-gS-\kappa(b-\alpha). \tag{2.1c}$$

Here, $\gamma_\parallel$ and $\gamma_\perp$ are the homogeneous longitudinal and transverse atomic relaxation rates, $\kappa=cT/L$ (c is the velocity of light) being the cavity half width; $\sigma=\frac{1}{2}(N_1-N_2)$ where N_1 and N_2 are, respectively, the lower and the upper atomic level populations; b is proportional to the transmitted electric field amplitude ($E_T=\sqrt{T}b$) and g is the atom-field coupling constant.

In the remainder of this work, we consider the limit $\kappa \ll \gamma_\parallel, \gamma_\perp$ (this corresponds to the good-quality-cavity limit referred to earlier). The atoms follow the field motion adiabatically and decay rapidly to their stationary state. Hence, we may set $\dot{S}=0=\dot{\sigma}$ in (2.1) and obtain an equation of motion for the transmitted field amplitude

$$\dot{x}=\kappa[y-x-2Cx/(1+x)]. \tag{2.2}$$

Here we have defined[2(b),2(e)]

$$C=g^2N/2\kappa\gamma_\perp, \tag{2.3}$$

$$y=\alpha/\sqrt{N_s}\ , \quad x=b/\sqrt{N_s}\ , \tag{2.4}$$

where

$$N_s=\gamma_\parallel\gamma_\perp/4g^2. \tag{2.5}$$

y and x are seen to be proportional to the incident and transmitted field amplitudes, respectively, N_s being the saturation photon number. The static behavior of the system is described by the state equation

$$y=x+\frac{2Cx}{(1+x^2)}, \quad x\in[0,\infty]. \tag{2.6}$$

Equation (2.6) is plotted in Fig. 1 for a parameter value $C=8$. It is seen that a bistable solution exists for $y_m<y<y_M$ for which the function in (2.6) takes on a relative maximum at $(x_M, y_M)\equiv(1.158\,941\,6, 9.072\,690\,2)$ and a relative minimum at $(x_m, y_m)\equiv(3.557\,647\,2, 7.725\,690\,3)$. It should be pointed out that for $C=0$ in (2.6), we obtain a straight line $y=x$. This is commonly referred to as the "one-atom" solution in resonance fluorescence.[2(b),14] For $C>4$, atomic cooperative effects come into play, leading to the first-order-like phase transition seen in Fig. 1. We see that for a range of the control parameter $y_m<y<y_M$, we find three steady states for the transmitted field. The steady-state values of x corresponding to those segments of the

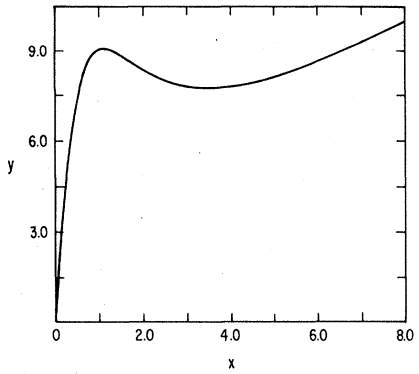

FIG. 1. Steady-state behavior of the transmitted field amplitude (x) as a function of the control parameter (y) for $C=8$.

curve having negative slope are unstable. The lower left portion of the curve is commonly referred to as the cooperative branch.[2(b)] For $x \to y > y_M$ the curve approximates the single-atom case referred to above.

In order to describe fluctuations in this system in general, we have to make use of the methods of quantum statistical mechanics.[2(e),6,7] For the description of the amplitude fluctuations, we follow a more phenomenological approach as pioneered by the work of Ref. 11. Assuming the phase of the transmitted field to be locked in to the phase ($\phi=0$) of the real, positive, incident field, we may derive the following (Ito-)stochastic differential equation[11] for the real amplitude fluctuations $x(t)$,

$$dx(t)=\kappa\left(y-x-\frac{2Cx}{1+x^2}\right)dt + \left(\frac{C}{N_s}\right)^{1/2}\frac{x}{1+x^2}\,dW\,, \tag{2.7}$$

with $dW(t)$ denoting the standard Wiener process increment. In writing (2.7) we assume that the fluctuations in $x(t)$ are rapid enough to be modeled as a white noise and manifest themselves as a white-noise fluctuation in the parameter C. To make contact with the microscopic approach, we set the variance of the C fluctuation equal to $(C/N_s)^{1/2}$ in (2.7). Introducing the dimensionless time $t \to \kappa t$ we have from (2.7), a Fokker-Planck equation for the rate of change of the probability $P(x, t)$:

$$\frac{\partial P(x,t)}{\partial t}=-\frac{\partial}{\partial x}\left[\left(y-x-\frac{2Cx}{1+x^2}\right)P(x,t)\right] + q\,\frac{\partial^2}{\partial x^2}\left[\left(\frac{x}{1+x^2}\right)^2 P(x,t)\right], \tag{2.8a}$$

where we set

$$q=C/2N_s\,. \tag{2.8b}$$

The Fokker-Planck equation (2.8) is defined on the state space $x(t)\in(0,\infty)$ and its solution is thus subject to boundary conditions. For our problem the physical boundary condition is that no probability is lost at the boundary $x=0$ ($x\equiv 0$, reflecting boundary). As a consequence any solution $P(x, t)$, in particular the conditional probability, satisfying the Fokker-Planck equation (2.8a) is subject to the normalization condition on the interval $(0,\infty)$; i.e.,

$$\int_0^\infty P(x,t)dx=1\,. \tag{2.9}$$

Further, the probability "current" as defined by the Fokker-Planck equation (2.8a) must vanish at $x=0$ and the diffusion term in (2.8a) should also be zero at this point [as is readily seen to be the case in (2.8a)], thereby implying the existence of a natural boundary at $x=0$.

Equation (2.8a) leads to the stationary solution

$$P_s(x)=\frac{1}{Z}\exp\left(-\frac{\bar{U}(x)}{q}\right), \tag{2.10}$$

Z being a normalization constant corresponding to the interval $(0,\infty)$. It must be pointed out here that the nonlinear diffusion term in (2.8) [which is a result of the multiplicative nature of the stochastic process (2.7)] makes it impossible for one to guess the "true" nonthermodynamic potential $\bar{U}(x)$ from the semiclassical deterministic equation. This is in contrast to the well-known situation for a single-mode laser in which the (delta-correlated) noise term enters the deterministic equation additively.[15] This nonlinear diffusion term reflects the influence of a quantum-statistical foundation which is a necessity for this problem. The potential $\bar{U}(x)$ for our problem is given by[2(e)]

$$\bar{U}(x)=\frac{y}{x}+(x-y)^2+Cx^2-\frac{x^3y}{3}+\frac{x^4}{4} + (2C+1)\ln x-2q\ln\left(\frac{1+x^2}{x}\right). \tag{2.11}$$

In general, the probability $P_s(x)$ may possess different extrema, these being given by the real positive roots of the polynomial equation,[11(a)]

$$(y-x)(1+x^2)^4-2Cx(1+x^2)^3-2qx(1-x^2)=0\,. \tag{2.12}$$

It is apparent from (2.12) that the range of the external control parameter, $y_m^{\text{Stoch}} < y < y_M^{\text{Stoch}}$, for which the stationary probability has three extrema, depends on the parameter q. It is only in the $q \to 0$ (i.e., $N \to \infty$) limit that the range of y^{Stoch} corresponding to a bimodal probability distribution agrees with the corresponding range of y for which Eq. (2.6) has three roots. In this context let us stress that the bimodal form of the probability $P_s(x)$ does not imply that the system shows metastability. In

other words, one cannot conclude from the bimodal form that a first-order phase transition actually has taken place between different locally stable steady states. Such a transition is characterized by a rate constant $\lambda_x = 1/T_x$ for the fluctuation relaxation between the stable and metastable state which undergoes, as a function of the *system size*, a softening transition.[16] Indeed, it has been shown[11(a)] that for

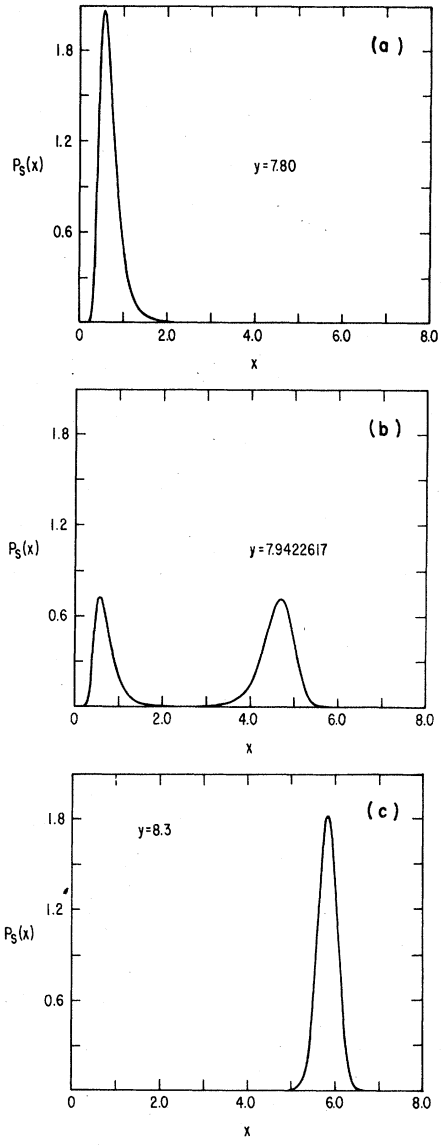

FIG. 2. (a) The stationary probability distribution $P_s(x)$ of the transmitted field for $C=8$, $q=1$, and $y=7.8$. (b) The stationary probability distribution $P_s(x)$ of the transmitted field for $C=8$, $q=1$, and $y=7.942\,261\,7\ldots$. The distribution is bimodal with peaks centered around the deterministically stable values. (c) The stationary probability distribution $P_s(x)$ of the transmitted field for $C=8$, $q=1$, and $y=8.3$, corresponding to the single-atom branch.

$C \leq 4$ one may obtain a bimodal stationary probability (through a suitable choice of the variance parameter of the fluctuations in C), whereas it is well known from the microscopic theory that, physically, the system may be bistable only for $C>4$. Figure 2 shows the shape of the stationary probability for different values of the control parameter y. It is seen to be asymmetric for lower y values, indicating a strongly non-Gaussian behavior. The two locally stable steady states occur with equal probability for $y \approx 7.942\ldots$. Due to the nonconstant diffusion term in (2.8), this value does not coincide[2(e)] with the thermodynamic-Maxwell-rule value $\bar{y}=8.16$ which is obtained by requiring the areas enclosed by $y(x)$ and the line $y=\bar{y}$ to be equal.

In Fig. 3, we plot the stationary statistical mean value $\langle x\rangle$ and the normalized variance

$$\frac{\langle(\delta x)^2\rangle}{\langle x\rangle^2} \equiv \frac{\langle(x-\langle x\rangle)^2\rangle}{\langle x\rangle^2} . \tag{2.13}$$

The mean value $\langle x\rangle$ exhibits a first-order-like phase-transition behavior with a narrow transition region, the gradient of the curve for $\langle x\rangle$ in the transition region providing a measure for the time scale of the fluctuations between the metastable and stable state.

Let us now return briefly to Eq. (2.11) and examine the scaling of the different terms with respect to the number of atoms N (i.e., the system size). Noting that the coupling constant g is proportional to $N^{-1/2}$ we find

$$b \propto N^{1/2}, \quad N_s = \gamma_{\parallel} N/8C\kappa \propto N, \quad q = \frac{4C^2\kappa}{\gamma_{\parallel} N} \propto N^{-1}, \tag{2.14}$$

C being independent of N. This scaling is reflected in the form for the stationary probability $P_s(x)$ de-

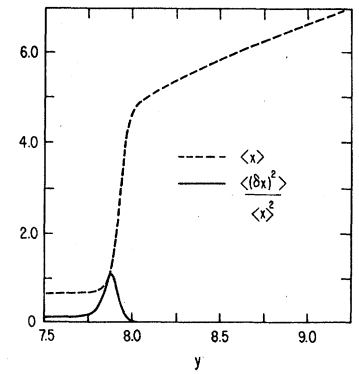

FIG. 3. Statistical mean value $\langle x\rangle$ of the transmitted field (dashed curve) and normalized variance $\langle(\delta x)^2\rangle/\langle x\rangle^2$ (solid curve) as functions of the control parameter (y) for $C=8$, $q=1$.

fined in (2.10):

$$P_s(x,\Omega)=\frac{1}{Z}\exp\{-\Omega[\Phi(x)+O(1/\Omega)]\}, \qquad (2.15)$$

where $\Omega=1/q\propto N$ is a measure of the system size so that the $O(1/\Omega)$ term in the exponent refers to the last term on the right-hand side of (2.11), $\Phi(x)$ referring to the remaining terms in (2.11). Let us consider the ratio of the stationary probabilities P_s at two different points:

$$R=\frac{P_s(x_1,\Omega)}{P_s(x_2,\Omega)}$$
$$=\exp\{-\Omega[\Phi(x_1)-\Phi(x_2)+O(1/\Omega)]\}. \qquad (2.16)$$

As $\Omega\to\infty$ on the x scale, this quantity may become infinite or vanish, except at $\Phi(x_1)=\Phi(x_2)$. Let us consider a small fluctuation $\Delta x=O(1/\Omega)$ about some value x_0. Then we may write

$$R=\frac{P_s(x_0+\Delta x,\Omega)}{P_s(x_0,\Omega)}$$
$$=\exp[-\Omega\Delta x\Phi'(x_0)+O(1/\Omega)],\quad \Delta x=O(\Omega^{-1}). \qquad (2.17)$$

The behavior of R about a maximum $\bar{x}$ of $P_s(x)$ (i.e., a minimum of the potential $\bar{U}$) is obtained by setting $\Phi'(\bar{x})=0$ and $\Phi''(\bar{x})>0$, with $\beta=\sqrt{\Omega}\,x\propto b$:

$$\frac{P_s(\bar{\beta}+\Delta\beta)}{P_s(\bar{\beta})}=\exp\left[-\frac{(\Delta\beta)^2}{2}\Phi''(\bar{x})+O\left(\frac{1}{\sqrt{\Omega}}\right)\right]$$
$$\Delta\beta=O(1). \qquad (2.18)$$

Hence, $P_s(b)$ is a Gaussian on the $(b-\bar{b})$ scale. whereas on the x scale it displays a δ-function behavior in the $\Omega\to\infty$ limit. We now investigate the change in the height of the probability P_s at the global maximum as a function of Ω. From (2.18) we find

$$\frac{P_s(\bar{x}+\Delta x,\Omega_2)}{P_s(\bar{x}+\Delta x,\Omega_1)}\sim\left(\frac{\Omega_2}{\Omega_1}\right)^{1/2}\exp[-(\Omega_2-\Omega_1)\Phi''(\bar{x})(\Delta x)^2/2]$$
$$\approx\left(\frac{\Omega_2}{\Omega_1}\right)^{1/2}\exp\{-(\Omega_2-\Omega_1)\times[\Phi(\bar{x}+\Delta x)-\Phi(\bar{x})]\}. \qquad (2.19)$$

At the maximum itself we find

$$\frac{P_s(\bar{x},\Omega_2)}{P_s(\bar{x},\Omega_1)}\sim\left(\frac{\Omega_2}{\Omega_1}\right)^{1/2}. \qquad (2.20)$$

We conclude this section with a more detailed discussion of the quantum-statistical foundation of the Fokker-Planck model (2.8) for the amplitude fluctuations. Such a discussion has been given previously[2(e)] for the stationary behavior. It was found that the difference between the stationary solution (2.10) and the exact solution $P_s^e(x)$ obtained from a full quantum-statistical treatment is not important. The exact solution $P_s^e(x)$ vanishes identically for $x>y$, expressing the fact that the transmitted field can never exceed the incident field. Our approximation in Eq. (2.10) yields for $x>y$ a finite but vanishingly small value as may be seen from Fig. 2. The approximate validity of the Markovian description in (2.8) for the dynamical behavior of the amplitude fluctuations is based on the assumption that the phase fluctuations occur sufficiently rapidly that we may eliminate the phase variable adiabatically in a master equation giving $x(t)$ the Markovian description of (2.8). In a corresponding Langevin picture for $z(t)=(x(t),\phi(t))$, this amounts to setting $\dot{\phi}=0$, which then yields the assumed phase-locking description ($\phi=0$) used here. In principle, the *correct* stationary behavior of the amplitude fluctuations may be obtained by performing an exact coarse graining in the master equations for the joint process $z(t)=(x(t),\phi(t))$.[2(e)] However, this would yield a non-Markovian description for $x(t)$ in which the aged conditional probability of the (non) stationary process $x(t)$ depends in a nonlinear way[12] on the initial state $x(0)$. A linear stability analysis of the complex-valued mean-field equations gives

$$\lambda_\phi=1+2C/(1+x^2), \qquad (2.20')$$

$$\lambda_x=\frac{dy(x)}{dx}=1+2C\,\frac{1-x^2}{(1+x^2)^2}, \qquad (2.20'')$$

where λ_ϕ and λ_x are the normal-mode frequencies of the phase and amplitude, respectively. Figure 4 shows the behavior of λ_x as a function of y for $C=8$. For $y\ll C$, (2.20) gives

$$\lambda_\phi\approx\lambda_x \qquad (2.21)$$

and for $y\gg y_M$ we get

$$\lambda_\phi\approx\lambda_x=1, \qquad (2.22)$$

indicating that the phase-locking assumption may be invalid. However, for our chosen set of parameters, $C=8$ and $y\in(7.5,9.25)$, we find from (2.20)

$$\lambda_x\approx\tfrac{1}{2}\lambda_\phi. \qquad (2.23)$$

The expressions (2.20) give correct estimates for the physically relevant time scales only for a set of control parameters $\{y\}$ describing a Gaussian behavior of the fluctuations. In the transition region (which we consider in this paper), λ_x undergoes a system-size-dependent softening transition[16]

$$\lambda_x\sim O(e^{-k\Omega}), \qquad (2.24)$$

where k is a constant, giving $\lambda_\phi\gg\lambda_x$ (see also Sec. V). Hence, we can conclude that for our chosen set of parameters the adiabatic elimination of the

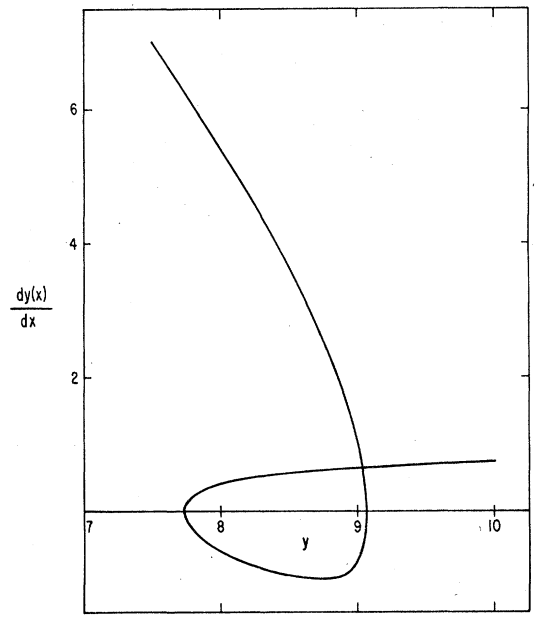

FIG. 4. Slope of the deterministic curve (Fig. 1) as a function of the control parameter for $C=8$. The ordinate is equal to the normal-mode frequency of the amplitude fluctuations [see Eq. (2.20'')].

phase variable is sufficiently justified in order to model the amplitude fluctuations via the Markovian Fokker-Planck equation (2.8).

III. LINEAR-RESPONSE THEORY

We consider the linear response of our system to a small additional coherent resonant classical field $\alpha^{\rm ext}(t)$ where it will be assumed that the nonstationary amplitude fluctuations in the presence of this perturbation remain Markovian. It readily follows from Eq. (2.7) (with α replaced by $\alpha+\alpha^{\rm ext}$) that the total perturbed system is described by the stochastic operator

$$\Gamma(t)=\Gamma_0+\Gamma^{\rm ext}(t)=\Gamma_0-F^{\rm ext}\frac{d}{dx}\ , \tag{3.1}$$

where

$$F^{\rm ext}(t)=\alpha^{\rm ext}(t)/\sqrt{N_s}\ . \tag{3.2}$$

Here, Γ_0 is the Fokker-Planck operator defined by Eq. (2.8):

$$\Gamma_0\equiv-\frac{\partial}{\partial x}\left[\left(y-x-\frac{2Cx}{1+x^2}\right)\right]+q\frac{\partial^2}{\partial x^2}\left(\frac{x}{1+x^2}\right)^2, \tag{3.3}$$

so that the presence of the additional signal is manifested only in the drift term as seen from (3.1) and (3.3). In terms of (3.1), we may cast the Fokker-Planck equation for the total perturbed system in the operator form

$$\frac{\partial\hat{P}(t,x)}{\partial t}=[\Gamma_0+\Gamma^{\rm ext}(t)]\hat{P}(x,t)$$
$$=\Gamma(t)\hat{P}(x,t)\,. \tag{3.4}$$

To first order in $F^{\rm ext}$, the solution of (3.4) is

$$\hat{P}(x,t)=P_s(x)-\int_0^t R_0(t-s)F^{\rm ext}(s)\left(\frac{d}{dx}P_s(x)\right)ds\,, \tag{3.5a}$$

where

$$R_0(\tau)=e^{\Gamma_0\tau}$$

with kernel (3.5b)

$$R_0(x,y;\tau)=\exp(\Gamma_0\tau)\delta(x-y)$$

is the unperturbed propagator.

Let $x(t)$ be a variable of interest in the system [in the present case, $x(t)$ is the transmitted field amplitude]. Then, the response of $x(t)$ to the perturbation is defined as the change in its mean value under the perturbation. This is written as

$$\langle\delta x(t)\rangle=\langle x(t)\rangle^{\rm perturbed}-\langle x\rangle_s\,. \tag{3.6}$$

The mean values in (3.6) are evaluated using the appropriate probability functions $\hat{P}(x,t)$ or $P_s(x)$. Then we find from (3.5a), for the linear response,

$$\langle\delta x(t)\rangle=\int x[\hat{P}(x,t)-P_s(x)]dx$$
$$=\int_0^t\chi(t-s)F^{\rm ext}(s)ds\,, \tag{3.7}$$

where we have defined a response function,

$$\chi(t)=-\theta(t)\iint xR_0(x,y;t)\frac{d}{dy}P_s(y)dy\,dx\,, \tag{3.8}$$

$\theta(t)$ being the step function. Note that $\int\Gamma^{\rm ext}(t)P_s(x)dx=0$, since the perturbation $\Gamma^{\rm ext}(t)$ cannot change the normalization of the probability function. We define the state function $\phi(x)$:

$$\phi(x)=\frac{d}{dx}\ln P_s(x)\,. \tag{3.9}$$

The response function $\chi(t)$ may now be expressed in terms of a generalized fluctuation-dissipation relation,[12(c),17]

$$\chi(t)=-\theta(t)\langle\delta x(t)\phi(x(0))\rangle_s\,. \tag{3.10}$$

The function $\phi(x)$ may be calculated for this case, using (2.10) and (2.11):

$$\phi(x)=-\frac{1}{q}\left(x^3-x^2y+2x(1+C)\right.$$
$$\left.+\frac{2C+1}{x}-\frac{y}{x^2}+2q\frac{1-x^2}{x(1+x^2)}\right), \tag{3.11}$$

where we have omitted constant terms due to the structure of (3.10). It should be noted that the

average $\langle \cdots \rangle_s$ is over the unperturbed steady-state, joint-probability distribution. In the following section we introduce the method of continued fractions which will be used ultimately to calculate the complex-valued Laplace transform of $\chi(t)$ (this quantity is referred to as the generalized susceptibility).

IV. DYNAMICAL CORRELATIONS

In this section we describe a calculation scheme for time-homogeneous correlations $A(t)$ of a stationary Markov process $x(t)$ with stochastic operator Γ (as defined in Sec. III). We define

$$A(\tau) = \langle g(x(\tau)) f(x(0)) \rangle = \int\int g(x) R_0(x, y; \tau) f(y) P_s(y) dy\, dx . \tag{4.1}$$

Expanding $A(\tau)$ in a Taylor series we have,

$$A(\tau) = \sum_{n=0}^{\infty} \frac{p_n}{n!} \tau^n , \quad \tau > 0 , \tag{4.2}$$

where

$$p_n = \left. \frac{d^n A(\tau)}{d\tau^n} \right|_{\tau = 0^+} \tag{4.3a}$$

$$= \int_0^{\infty} g(x) (\Gamma^n f P_s)(x) dx \tag{4.3b}$$

$$= \langle [(\Gamma^+)^n g][x(0)] f(x(0)) \rangle . \tag{4.3c}$$

Note that in Eq. (4.3b) the integration limits for x take care [with P_s normalized in $(0, \infty)$] automatically, of the reflecting boundary condition at $x = 0$. Equation (4.3c) expresses the moment p_n as a *stationary expectation*, Γ^+ denoting the transpose operator with kernel $\Gamma^+(x, x') = \Gamma(x', x)$. The Laplace transform of Eq. (4.2) is,

$$A(\omega) = \lim_{\epsilon \to 0} \int_0^{\infty} A(\tau) e^{(i\omega - \epsilon)\tau} d\tau , \quad \epsilon > 0 \tag{4.4}$$

and may be written as a high-frequency expansion (generally an asymptotic series)

$$A(\omega) = \sum_{n=0}^{\infty} \frac{p_n}{z^{n+1}} , \quad z = -i\omega . \tag{4.5}$$

We now perform an analytic continuation of this series using a continued-fraction representation for $A(\omega)$ (Refs. 13, 17, 18):

$$A(\omega) = \cfrac{c_1}{z + \cfrac{c_2}{1 + \cfrac{c_3}{z + \cfrac{c_4}{1 + \cdots}}}} \tag{4.6}$$

$$= \cfrac{b_1}{z + a_1 - \cfrac{b_2}{z + a_2 - \cfrac{b_3}{z + a_3 + \cdots}}} . \tag{4.7}$$

The continued-fraction coefficients $\{c_n\}$ may be calculated from the set of moments $\{p_n\}$ in a very efficient manner, by use of the recursive algorithm presented in Refs. 17 and 18. The explicit expressions for the first six coefficients are given in the Appendix. In terms of the coefficients $\{c_n\}$, the coefficients $\{b_n\}$ and $\{a_n\}$ of the contracted form in (4.7) are simply given by

$$b_1 = c_1 , \quad a_1 = c_2 \tag{4.8a}$$

$$b_{n+1} = c_{2n} c_{2n+1} , \quad a_{n+1} = c_{2n+1} c_{2n+2} . \tag{4.8b}$$

An alternative procedure for evaluating the coefficients in (4.7) has been used by Grossmann and Schranner[13] using projection-operator techniques.

The lowest-order truncation of Eq. (4.6) leads to the simple Lorentzian

$$A^{(1)}(\omega) = \frac{b_1}{-i\omega + a_1} \tag{4.9}$$

or

$$A^{(1)}(\tau) = b_1 e^{-a_1 \tau} , \quad \tau > 0 . \tag{4.10}$$

Truncation of (4.6) at higher orders ($n > 2$) allows us to take memory effects[13] into account; these effects result from the nonlinear coupling of the macrovariables yielding a deviation from a simple Lorentzian relaxation behavior (these memory effects are not to be confused with those arising in a stochastic process due to the non-Markovian behavior of the system). Setting $b_n (n \geq 3) = 0$ in (4.7), we obtain the lowest-order contribution to the memory effects:

$$A^{(2)}\omega = b_1 \left(-i\omega + a_1 - \frac{b_2}{-i\omega + a_2} \right)^{-1} = b_1 \left(\frac{1 - \alpha}{-i\omega + \lambda_1} + \frac{\alpha}{-i\omega + \lambda_2} \right) , \tag{4.11}$$

where

$$\lambda_{1,2} = \tfrac{1}{2} \{ a_1 + a_2 \mp [(a_1 - a_2)^2 + 4b_2]^{1/2} \} , \tag{4.12}$$

$$\alpha = \frac{\lambda_2 - a_2}{\lambda_2 - \lambda_1} . \tag{4.13}$$

Hence, the deviation of α from zero reflects the influence of the memory effects. In this context, it should be stressed that the actual values of the poles λ_1 and λ_2, as well as α, become renormalized by higher-order truncation approximations. Thus, the expressions in (4.12) and (4.13) may be looked upon as the *bare* memory coefficients.

V. CALCULATIONS

In order to evaluate the continued-fraction coefficients $\{c_n\}$ in Eq. (4.7), we must first calculate the static moments $\{p_n\}$. The stationary probability (2.10) is seen to vanish as $x \to 0^+$:

$$P_s(x=0^+) = \lim_{x\to 0} \exp[-(y/qx) + O(\ln x)] = 0 . \quad (5.1)$$

Using Eq. (3.3), the transposed operator Γ_0^+ in (4.3c) is then given by

$$\Gamma_0^+ = \left(y - x - \frac{2Cx}{1+x^2}\right)\frac{d}{dx} + q\,\frac{x^2}{(1+x^2)^2}\,\frac{d^2}{dx^2} . \quad (5.2)$$

Moreover, due to the one-dimensional character of the amplitude x, the operator Γ_0^+ is symmetric with respect to the scalar product (f,g) defined by

$$(f,g) = \int f(x)g(x)P_s(x)dx \equiv \langle fg\rangle_s . \quad (5.3)$$

In other words, we have the property

$$\langle(\Gamma_0^+ f)g\rangle = (f,\Gamma_0^+ g) = \langle f(\Gamma_0^+ g)\rangle_s . \quad (5.4)$$

This property considerably simplifies the calculation of the static moments $\{p_n\}$ in the form given by Eq. (4.3c) since we readily observe

$$p_{n+m} = ((\Gamma_0^+)^{n+m} g, f) = ((\Gamma_0^+)^n g, (\Gamma_0^+)^m f), \quad (5.5)$$

m and n denoting integers. The relation (5.5) is also very useful for checking the accuracy of the numerical calculations. In the following subsections, we discuss in detail the calculations of the autocorrelation function of amplitude fluctuations (together with the associated spectrum), and the evaluation of the response function and complex susceptibility introduced in Sec. III.

A. The spectrum of amplitude fluctuations

From the autocorrelation $S(\tau)$ of the amplitude fluctuations,

$$S(\tau) = S(-\tau) = \langle \delta x(\tau)\delta x(0)\rangle_s , \quad (5.6)$$

we obtain the spectral function $S(\omega)$:

$$S(\omega) = \int_{-\infty}^{\infty} S(\tau)e^{i\omega\tau}d\tau = 2\,\mathrm{Re}\bar{S}(\omega) \geq 0 , \quad (5.7a)$$

where

$$\bar{S}(\omega) = \int_0^{\infty} S(\tau)e^{i\omega\tau}d\tau . \quad (5.7b)$$

The set of static moments $\{s_n\}$ corresponding to the autocorrelation $S(\tau)$ are calculated via Eq. (5.5) with $f(x) = g(x) = x - \langle x\rangle$. Since Γ_0 satisfies the symmetry property (5.4), the sequence of moments $\{s_n\}$ may be shown to form a Stieltjes sequence.[10] Hence, the continued-fraction coefficients $\{c_n^{(s)}\}$ corresponding to the autocorrelation function are positive semidefinite, i.e.,

$$c_n^{(s)} \geq 0 , \quad n = 1,2,\ldots . \quad (5.8)$$

This allows us to construct *a posteriori* error bounds[10] which in our case read

$$|S(\omega) - S^{(n)}(\omega)| \leq 2\,|\bar{S}^{(n)}(\omega) - \bar{S}^{(n-1)}(\omega)| , \quad (5.9)$$

where $S^{(n)}, \bar{S}^{(n)}$ denote the nth-order truncated continued-fraction approximations to (4.6) obtained by setting $c_{n+1} = c_{n+2} = \cdots = 0$.

Using Eq. (5.5) and the relations given in the Appendix, we find for the coefficients b_1, a_1, b_2, a_2 of the contracted form (4.7) the explicit expressions

$$b_1 = \langle(\delta x)^2\rangle , \quad (5.10a)$$

$$a_1 = 1 - \frac{2C}{b_1}\left(\langle x\rangle\left\langle\frac{x}{1+x^2}\right\rangle - \left\langle\frac{x^2}{1+x^2}\right\rangle\right) , \quad (5.10b)$$

$$b_2 = -1 - \frac{4C}{b_1}\left\langle\frac{x\delta x}{1+x^2}\right\rangle - \frac{4C^2}{b_1^2}\left\langle\frac{x\delta x}{1+x^2}\right\rangle^2 + \frac{1}{b_1}\left\langle\left(y - x - \frac{2Cx}{1+x^2}\right)^2\right\rangle , \quad (5.10c)$$

$$a_2 = \frac{1}{b_1 b_2}\left[-a_1 b_1 b_2 - a_1\left\langle\left(y - x - \frac{2Cx}{1+x^2}\right)\right\rangle^2 + \left\langle\left(y - x - \frac{2Cx}{1+x^2}\right)^2\left(1 + 2C\,\frac{1-x^2}{(1+x^2)^2}\right)\right\rangle + 4Cq\left\langle\left(y - x - \frac{2Cx}{1+x^2}\right)\frac{x^5 - 3x^3}{(1+x^2)^5}\right\rangle\right] , \quad (5.10d)$$

where we recall that $\delta x \equiv x - \langle x\rangle$ and the averages above are taken with respect to the stationary probability distribution $P_s(x)$ defined in (2.10).

The numerical calculations have been performed by use of a Romberg-integration scheme requiring for all integrals a relative accuracy of 10^{-8}. The results of the numerical calculations using two different parameter values of the system size Ω are given in Figs. 5–8.

In Figs. 5(a) and 5(b) we have plotted, as functions of the external control parameter (y), the exponential decay rate a_1 [defined in (4.7)–(4.9)] and the bare-memory-relaxation rate λ_1 defined in (4.12). Note that due to the fact that $\bar{S}(\omega)$ constitutes a Stieltjes continued fraction, the relaxation rates denote upper bounds[18] to the *first* nonzero eigenvalue λ_x of the Fokker-Planck operator Γ_0:

$$a_1 \geq \lambda_1 \geq \lambda_1^{\mathrm{ren}} \geq \lambda_x > 0 , \quad (5.11)$$

where "ren" stands for a renormalized value. The relaxation rates show the critical slowing down in the transition region around $y = 7.9\ldots$. For values of the control parameter $y \gtrsim 8.1$, where the stationary probability $P_s(x)$ has its main weight on the single-atom branch, we find that the relaxation rates a_1 and λ_1 are remarkably close in value to the Gaussian relaxation parameter in Fig. 4 given by the gradient of the slope of the state equation (2.6). For our chosen set of parameters (q, C), the values of a_1 and λ_1 corresponding to the stable state on the lower cooperative branch ($y \lesssim 7.75$) are found to lie below the Gaussian values. Such a behavior is expected because the influence of nonlinear corrections, stemming from the nonlinear

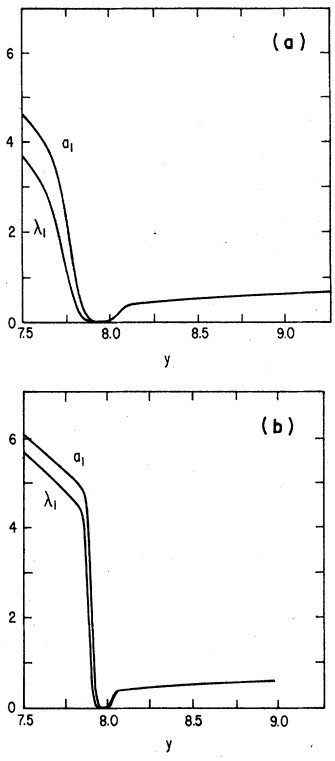

FIG. 5. (a) The exponential decay rate a_1 [see Eqs. (4.7)–(4.9)] and the bare-memory relaxation rate λ_1 [see Eq. (4.12)] for the spectrum of amplitude fluctuations with $q=1$ and $C=8$. (b) The exponential decay rate a_1 [see Eqs. (4.7)–(4.9)] and the bare-memory relaxation rate λ_1 [see Eq. (4.12)] for the spectrum of amplitude fluctuations with $q=0.4$ and $C=8$.

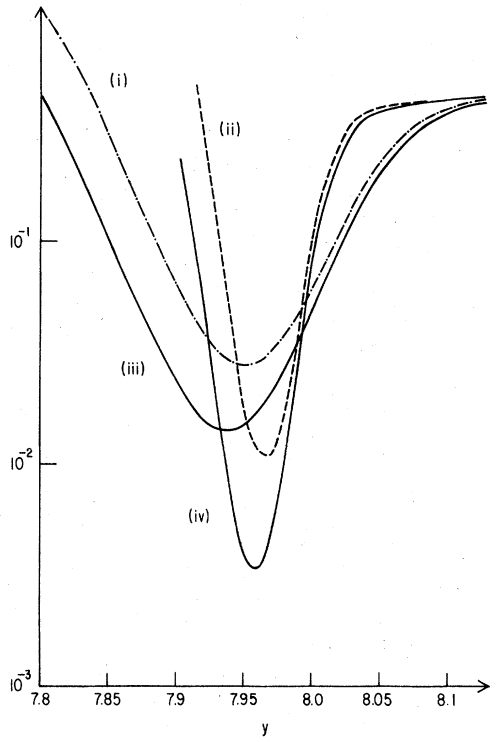

FIG. 6. Details of critical slowing-down behavior in the transition region corresponding to Figs. 5(a) and 5(b). Curves (i) and (ii) show the behavior of a_1 for $q=1$ and 0.4, respectively. Curves (iii) and (iv) show the slowing down of λ_1 for $q=1$ and 0.4, respectively.

drift and diffusion coefficients, to a linearized Fokker-Planck approximation around the steady state are more pronounced in the region of the cooperative branch. This behavior is already indicated in the *asymmetric* shape of the stationary probability P_s (see Fig. 2). Figure 6 shows in greater detail the critical slowing-down behavior in the transition region.

For our chosen sets of parameter values for C and q, the minimum values of the bare-memory relaxation rate λ_1 for small system size ($q \lesssim 1$) compare favorably with the values obtained through a first-passage-time relation.[19] The continued fraction parameter a_1 gives, away from the minimum, an estimate for the first nonzero eigenvalue that is too high. In this region, where the weight of the metastable state in the stationary probability becomes smaller (as y moves away from the point describing equal probability between the two locally stable states), the continued fraction technique tends to simulate the stochastics of a monomodel stationary probability behavior. The memory effects present in the bare-relaxation rate λ_1 or, more generally, λ_1^{ren}, correct this behavior and give smaller upper limits to the first nonzero eigenvalue. In this context, it is worthwhile to discuss the limits of applicability of the continued fraction method in the asymptotic limit of a large system size $\Omega \sim q^{-1}$. For a small q value, the ratio R of the probabilities for the metastable and stable state [see Eq. (2.16)] vanishes exponentially [except at the value of y such that $\phi(x_1)=\phi(x_2)$]. Thus, because the influence of the maxima of the metastable state in $P_s(x)$ vanishes exponentially, a *finite* continued-fraction approximation fails in the proper thermodynamic limit.[20] Moreover, the applicability of the continued-fraction method for small q values is limited in practice by numerical instabilities due to round-off errors.

The results for the bare-memory-strength parameter α are given in Fig. 7. There are two regions where the deviation from a simple Lorentzian ($\alpha=0$) is important. In between these regions where $\langle x \rangle$ changes approximately linearly from the cooperative branch to the high single-atom branch (see Fig. 3), α is small again. For larger system sizes, the maxima of α get closer to one another and the peaks become sharper, corresponding to a

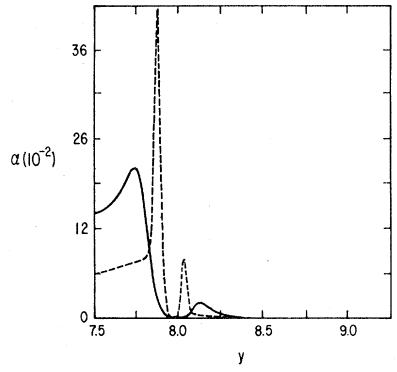

FIG. 7. The "bare"-memory strength parameter α [see Eq. (4.13)] for the spectrum of amplitude fluctuations with $C=8$ and $q=1$ (solid curve), $q=0.4$ (dashed curve).

sharpening of the transition. This behavior resembles that of a first-order chemical reaction discussed in Ref. 13(a). Note also that the values of α in the region with the stable state on the cooperative branch are dominantly larger than those on the high single-atom branch. This behavior once again reflects the deviation from a Gaussian-Markovian behavior for which $\alpha \equiv 0$. In Fig. 8, we show the second-order continued-fraction coefficient a_2. The graph shows a fluctuation around the transition region which becomes enhanced for increasing system sizes.

The spectrum $S(\omega)$ has been calculated via the continued-fraction representation of Eq. (4.6), with $\bar{S}(\omega)$ defined in (5.7b). In this context, it should be mentioned that the calculation scheme for the continued-fraction coefficients in terms of the static moments is not stable against round-off errors, in contrast to an algorithm for calculating the moments from a given set of continued-fraction coefficients, which is stable. Consequently, in order

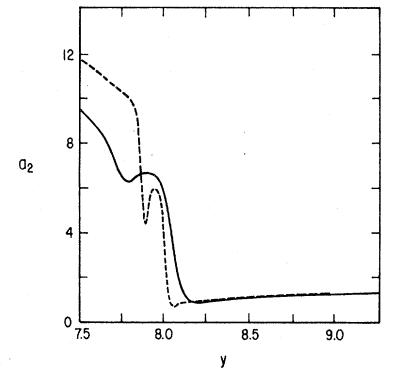

FIG. 8. The second-order continued-fraction coefficient a_2 for the amplitude fluctuations, as a function of the control parameter (y) for $C=8$ and $q=1$ (solid curve), $q=0.4$ (dashed curve).

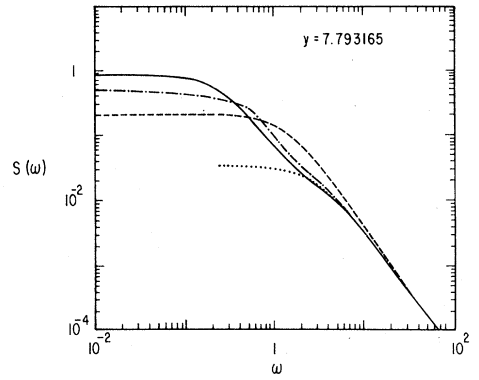

FIG. 9. The spectral density $S(\omega)$[Eq. (5.7a)] of the amplitude fluctuations for $y=7.793165\ldots$. The curves represent the result of truncating the continued-fraction expansion (4.6) at $n=2$ (dashed curve), $n=4$ (dashed and dotted curve), $n=6$ (solid curve), and $n=7$ (dotted curve), $C=8$, $q=1$.

to retain a relative accuracy of 10^{-8} for the numerical calculations, all derivatives stemming from expressions such as $[(\Gamma^+)^n g](x)$ have been calculated analytically. In this way we have evaluated the approximate spectral functions by calculating up to seven continued-fraction coefficients $c_i, i=1,\ldots,7$. The results of the numerical calculations of the spectral density are shown in Figs. 9 and 10. We note that an odd truncated-continued-fraction approximation to Eq. (4.6) has a poor convergence behavior for low frequencies ω. This may be understood from the corresponding pole representation. For n odd, we obtain with the pole frequency $\nu_1 \equiv 0$ and some general memory strength β,

$$A^{(\mathrm{odd})}(\omega) \propto \frac{1-\beta}{-i\omega} + \frac{\beta}{-i\omega+\nu_2} + \cdots , \tag{5.12}$$

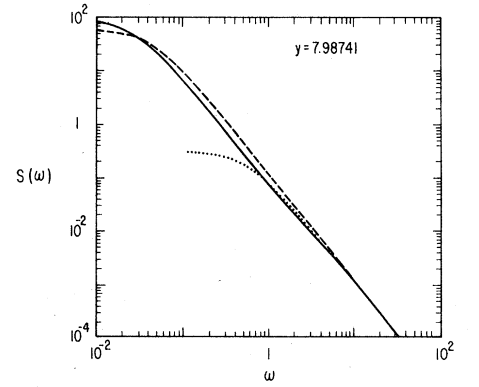

FIG. 10. The spectral density $S(\omega)$[Eq. (5.7a)] of the amplitude fluctuations for $y=7.987\,41\ldots$. The curves represent the result of truncating the continued-fraction expansion (4.6) at $n=2$ (dashed curve), $n=6$ (solid curve), and $n=7$ (dotted curve), $C=8$, $q=1$.

which yields for $\omega \ll 1$ a very small real part (or a very large imaginary part). Comparing the sixth-order truncated fraction [this corresponds to the third-order truncated fraction in the contracted form (4.7)] with the single Lorentzian obtained via the second truncated fraction, we see that the memory effects are most important for very small frequencies (in this regime, a small frequency perturbation is sensitive to the *long* time scale $\tau^{-1} \approx dy/d\langle x\rangle$ where the stochastic-state equation for $\langle x\rangle$ is plotted in Fig. 3). In this case we find from (4.11),

$$S(\omega) \approx 2b_1 \frac{1-\alpha^{\text{ren}}}{\lambda_1^{\text{ren}}}, \quad \omega < \lambda_1 . \tag{5.13}$$

The memory effects are also important for $\omega \lesssim \lambda_2$ where the influence of the superposition of a second Lorentzian L_2

$$L_2 \propto \frac{\alpha^{\text{ren}}\lambda_2^{\text{ren}}}{(\lambda_2^{\text{ren}})^2 + \omega^2} \tag{5.14}$$

becomes observable. Due to the small magnitude of the memory coefficient α (see Fig. 7), the influence of this second Lorentzian is somewhat suppressed but still quite perceivable in Fig. 9. The high-frequency tail shows the usual ω^{-2} characteristic.

B. The response function

The static moments $\{r_n\}$ corresponding to the response function [these are the analogs of the $\{p_n\}$ introduced in (4.2)] in Eq. (3.7) are calculated from the relation (5.5) with $g(x) \equiv x - \langle x\rangle_s$ and $f(x) \equiv -\phi(x)$, $\phi(x)$ being defined in (3.11). Since $f \neq g$, the continued-fraction representation for the complex-valued (polarization) susceptibility $\chi(\omega)$,

$$\chi(\omega) = -\int_0^\infty \langle \delta x(\tau)\phi(x(0))\rangle e^{i\omega\tau} d\tau \tag{5.15}$$

is, in general, not of the form of a rapidly convergent Stieltjes function. In the numerical calculations, we find once again for the relaxation frequencies $a_1, \lambda_1^{\text{ren}}$ calculated from the set of moments $\{r_n\}$ a critical slowing behavior. However, compared with the rapid convergence behavior observed for the spectral density $S(\omega)$, we find here a slower convergence rate. The "bare" memory coefficient α for this case is plotted in Fig. 11. It is seen that the memory strength in this case exhibits the same general behavior as observed for the spectral function (Fig. 7) with the difference that the two peaks are less enhanced. For larger y values, where the stable stationary state is on the single-atom branch, the values of α approach those for the autocorrelation. As mentioned earlier, the amplitude fluctuations in this region may be treated as a Gaussian-Markovian process to a good approximation. Hence, in the limit of a large system size, the response function $\chi(t)$ may be represented asymptotically as an ordinary fluctuation-dissipation theorem:

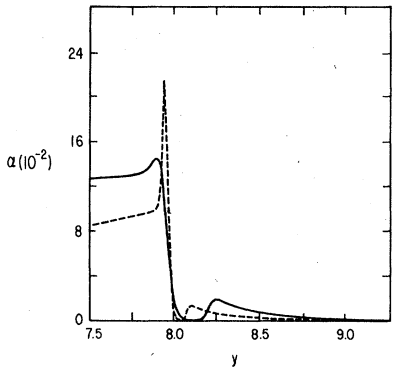

FIG. 11. The "bare"-memory strength parameter α corresponding to the response function with $C=8$ and $q=1$ (solid curve), $q=0.4$ (dashed curve).

$$\chi(t) \approx \theta(t) b_1^{-1} \langle \delta x(t)\delta x(0)\rangle . \tag{5.16}$$

The continued-fraction coefficient a_2 for this case is shown in Fig. 12. In Fig. 13 we plot the real and imaginary parts of the generalized susceptibility $\chi(\omega)$ for $y = 8.138\,489\ldots$. This y value corresponds to a region wherein the amplitude fluctuations are approximately Gaussian. In this case, we observe that the continued-fraction expansion (4.6) may be truncated at $n=2$ to a very high degree of accuracy (reflecting the near total absence of memory effects in this regime). Indeed, for a frequency $\omega = 0.0252$ for example, we obtain a percentage error of 1.7% when we truncate the continued fraction, Eq. (4.6), at $n=2$ rather than at $n=6$. We also find, in accordance with the statements made earlier in this section, that the real part of the susceptibility

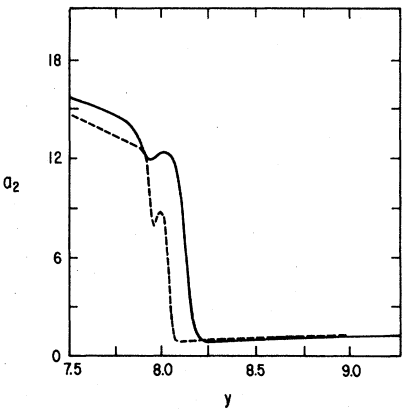

FIG. 12. The second-order continued-fraction coefficient a_2 for the response function with $C=8$ and $q=1$ (solid curve), $q=0.4$ (dashed curve).

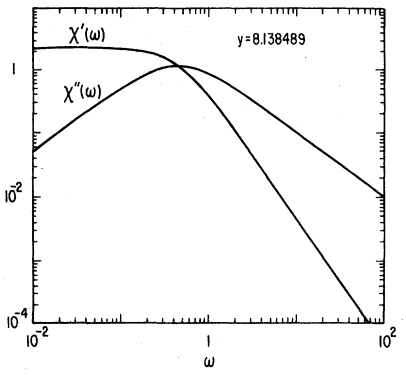

FIG. 13. The real part $[\chi'(\omega)]$ and imaginary part $[\chi''(\omega)]$ of the generalized susceptibility $\chi(\omega)$ [see Eq. (5.15)] for $y = 8.138489\ldots$. The amplitude fluctuations are approximately Gaussian and the continued-fraction expansion (4.6) may be truncated at $n = 2$ within the range of accuracy of this graph. In this case, $\chi(\omega)$ is given approximately by the fluctuation-dissipation theorem (5.16), $C = 8$, $q = 1$.

is almost coincident with $S(\omega)/2b_1$ (for $\omega = 0.0252$, the percentage difference between these quantities is 3.36% for $n = 2$ and 0.8% for $n = 6$).

To conclude this section, we briefly comment on the physical meaning of the susceptibility $\chi(\omega)$. It is well known[21] that the susceptibility is a measure of the response of the atoms to an externally applied electric field. In a linear theory (for not too strong fields), the polarization induced by an external field is proportional to the field, $\chi(\omega)$ being the constant of proportionality. In the system considered in this work, the additional small signal α^{ext} induces a change in the polarization S of the atoms in the cavity. The susceptibility calculated in this section is actually a measure of the atomic response to this additional field. Since we have assumed the incident field to be real (this is a consequence of the phase-locking assumption), we have $\chi^*(\omega) = \chi(-\omega)$.

ACKNOWLEDGMENTS

We thank Dr. W. C. Schieve and Mr. R. F. Gragg of the University of Texas at Austin for helpful discussions. The work of P.H. and A.R.B. was supported by the National Science Foundation under Grant No. CHE78-21460 and by a grant from Charles and Renée Taubman.

APPENDIX

The explicit expressions for the first six continued-fraction coefficients of Eq. (4.6) are expressed in terms of the stationary moments $\{p_n\}$ as

$$c_1 = p_0 , \tag{A1}$$

$$c_2 = -p_1/p_0 , \tag{A2}$$

$$c_3 = \frac{-p_2 p_0 + p_1^2}{p_0 p_1} , \tag{A3}$$

$$c_4 = \frac{p_0(p_1 p_3 - p_2^2)}{p_1(p_0 p_2 - p_1^2)} , \tag{A4}$$

$$c_5 = \frac{-p_0^2 p_1 p_2 p_4 + p_0 p_1^3 p_4 + p_0 p_1 p_2^3 + p_0^2 p_1 p_3^2 - 2 p_0 p_1^2 p_2 p_3}{p_0(p_1 p_3 - p_2^2)(p_0 p_2 - p_1^2)} , \tag{A5}$$

$$c_6 = -c_5 + \frac{p_0 p_3 - p_1 p_2}{p_0 p_2 - p_1^2} + \frac{(p_3 p_2^2 + p_0 p_3 p_4 + p_1^2 p_5 - p_0 p_2 p_5 - p_1 p_2 p_4 - p_1 p_3^2)}{(p_0 p_2 p_4 + 2 p_1 p_2 p_3 - p_2^3 - p_0 p_3^2 - p_1^2 p_4)} . \tag{A6}$$

[1] A. Szoke, Y. Daneu, J. Goldhar, and N. Kurnit, Appl. Phys. Lett. 15, 376 (1969).

[2] (a) S. L. McCall, Phys. Rev. A 9, 1515 (1974); (b) R. Bonifaccio and L. Lugiato, Opt. Commun. 19, 172 (1976); (c) C. Willis, *ibid.* 23, 151 (1977); 26, 62 (1978); (d) H. Carmichael and D. Walls, J. Phys. B 9, 1199 (1976); 10, L685 (1977); (e) R. Bonifaccio, M. Gronchi, and L. Lugiato, Phys. Rev. A 18, 2266 (1978); (f) L. Narducci, D. Feng, R. Gilmore, and G. Agarwal, *ibid.* 18, 1571 (1978); (g) R. Gragg, W. Schieve, and A. Bulsara, *ibid.* 19, 2052 (1979); (h) C. Bowden and C. Sung, *ibid.* 19, 2392 (1979).

[3] (a) H. Gibbs, S. McCall, and T. N. C. Venkatesan, Phys. Rev. Lett. 36, 1135 (1976); (b) T. N. C. Venkatesan and S. McCall, Appl. Phys. Lett. 23, 731 (1976).

[4] (a) F. Felber and J. Marburger, Appl. Phys. Lett. 23, 731 (1976); (b) P. Smith and E. Turner, *ibid.* 30, 280 (1977); (c) K. Jain and G. Pratt, Jr., *ibid.* 28, 719 (1977); (d) M. Okuda and K. Onaka, Jpn. J. Appl. Phys. 16, 303 (1977).

[5] (a) R. Bonifaccio and L. Lugiato, Lett. Nuovo Cimento 21, 505 (1978); (b) P. Meystre, Opt. Commun. 26,

277 (1978).
[6](a) L. Lugiato, Nuovo Cimento 50B, 89 (1979); (b) R. Bonifaccio and L. Lugiato, Phys. Rev. Lett. 40, 1023 (1978).
[7]G. Agarwal, L. Narducci, R. Gilmore, and D. Feng, Phys. Rev. A 18, 620 (1978); 20, 545 (1979).
[8](a) N. van Kampen, Can. J. Phys. 39, 551 (1961); (b) R. Kubo, K. Matsuo, and K. Kitahara, J. Stat. Phys. 9, 51 (1973).
[9](a) P. Hanggi, Z. Phys. B30, 85 (1978); (b) T. Kurtz, Stoch. Prob. Appl. 6, 223 (1978).
[10]P. Hanggi, Z. Naturforsch 33a, 1380 (1978).
[11](a) A. Bulsara, W. Schieve, and R. Gragg, Phys. Lett. 68A, 294 (1978); (b) F. Arecchi and A. Politi, Opt. Commun. 29, 361 (1978).
[12](a) P. Hanggi and H. Thomas, Z. Phys. B26, 85 (1977); (b) H. Grabert, P. Talkner, P. Hanggi, and H. Thomas, Z. Phys. B29, 273 (1978); (c) P. Hanggi and H. Thomas, Phys. Rep. C (in press).
[13](a) S. Grossmann and R. Schranner, Z. Phys. B30, 325 (1978); (b) S. Grossmann, Phys. Rev. A 17, 1123 (1978).
[14]B. Mollow, Phys. Rev. 188, 1969 (1969); H. Carmichael and D. Walls, J. Phys. B 9, 1199 (1976).
[15]See, e.g., H. Haken, *Synergetics* (Springer, Berlin, 1977).
[16]R. Landauer, J. Appl. Phys. 33, 2209 (1962); J. Langer, Ann. Phys. (N. Y.) 54, 258 (1969); H. Janssen, Z. Phys. 270, 67 (1974); H. Tomita, A. Ito, and H. Kidachi, Progr. Theor. Phys. 56, 786 (1976); I. Oppenheim, K. Shuler, and G. Weiss, Physica (Utrecht) 88A, 191 (1977).
[17]P. Hanggi, Helv. Phys. Acta 51, 202 (1978).
[18]P. Hanggi, F. Rosel, and D. Trautmann, Z. Naturforsch 33a, 402 (1978).
[19]K. Lindenberg, K. Shuler, J. Freeman, and T. Lie, J. Stat. Phys. 12, 217 (1975).
[20]This is an agreement with Ref. 13(a). However, we disagree with the conjecture stated therein that *other* poles of any finite continued fraction of the contracted form (4.7) also approach zero for small q. Such a behavior contradicts the theory of Stieltjes fractions giving in this case upper bounds for the relaxation frequencies (Ref. 18).
[21]See, e.g., R. Loudon, *The Quantum Theory of Light* (Clarendon, Oxford, 1973).